Received: 30 June 2022 | Revised: 12 September 2022 | Accepted: 8 November 2022

DOI: 10.1002/app.53444

RESEARCH ARTICLE

Journal of Applied Polymer Science WILEY

Virus removal from aqueous environments with polyelectrolyte coatings on a polypropylene fleece

Maiko Schulze | Chuanxiong Nie | Greta Hartmann | Philip Nickl | Michaël W. Kulka | Matthias Ballauff | Rainer Haag

Institute of Chemistry and Biochemistry, Freie Universität Berlin, Berlin, Germany

Correspondence
Rainer Haag, Institute of Chemistry and Biochemistry, Freie Universität Berlin, Takustr. 3, 14195, Berlin, Germany.
Email: haag@chemie.fu-berlin.de

Funding information
Bundesministerium für Bildung und Forschung, Grant/Award Number: 13GW0544E

Abstract

The adsorption of viruses from aqueous solution is frequently performed to detect viruses. Charged filtration materials capture viruses via electrostatic interactions, but lack the specificity of biological virus-binding substances like heparin. Herein, we present three methods to immobilize heparin-mimicking, virus-binding polymers to a filter material. Two mussel-inspired approaches are used, based on dopamine or mussel-inspired dendritic polyglycerol, and post-functionalized with a block-copolymer consisting of linear polyglycerol sulfate and amino groups as anchor (lPGS-*b*-NH_2). As third method, a polymer coating based on lPGS with benzophenone anchor groups is tested (lPGS-*b*-BPh). All three methods yield dense and stable coatings. A positively charged dye serves as a tool to quantitatively analyze the sulfate content on coated fleece. Especially lPGS-*b*-BPh is shown to be a dense polymer brush coating with about 0.1 polymer chains per nm^2. Proteins adsorb to the lPGS coated materials depending on their charge, as shown for lysozyme and human serum albumin. Finally, herpes simplex virus type 1 (HSV-1) and severe acute respiratory syndrome coronavirus type 2 (SARS-CoV-2) can be removed from solution upon incubation with coated fleece materials by about 90% and 45%, respectively. In summary, the presented techniques may be a useful tool to collect viruses from aqueous environments.

KEYWORDS

linear polyglycerol sulfate, mussel-inspired coatings, polyelectrolyte brushes, surface coatings, virus filters

1 | INTRODUCTION

The spread of the severe acute respiratory syndrome coronavirus type 2 (SARS-CoV-2) is still ongoing, with more than 500 million confirmed cases worldwide.[1,2]

A simple and efficient technique to monitor the occurrence of viruses and their spread in the population is to detect them in wastewater.[3] This method has been used for several virus species in the past, for example, norovirus,[4,5] hepatitis E,[6] or hepatitis A viruses.[7] Since

the global spread of SARS-CoV-2 began in 2020, the detection of that virus in wastewater has been of great interest as well.[8–10]

In the detection process, raw wastewater is collected at a wastewater treatment plant, the virus concentration is increased, and then the virus is quantified. Several methods have been used for concentration of viruses, including ultracentrifugation, precipitation with polyethylene glycol, ultrafiltration, or adsorption-elution.[3] The adsorption-elution method is among the most common techniques for sample concentration from wastewater.[11] It is based on the filtration of the analyte through a charged membrane and successive resuspension of the captured viruses with an eluent. Electrostatic interactions between the membrane and either viral spike proteins (enveloped viruses) or capsid proteins (non-enveloped viruses) lead to the retention of viral particles.

The detection of viruses from wastewater samples with the adsorption-elution method requires sample volumes in the range of 0.5–400 L.[3,12] These high amounts are necessary because of the very low virus concentration on the one hand, and the non-quantitative capture efficiency of the membranes on the other hand.[11,12] After the concentration by adsorption-elution, the virus concentration is often still too low for detection, making a secondary concentration step necessary, for example, additional precipitation with polyethylene glycol.[3,12] Thus, the overall process is laborious and costly, and a more efficient adsorption-elution method is required.

Membranes for the adsorption and elution of viruses are commonly made of charged materials, for example, a mixture of cellulose nitrate and cellulose acetate.[11] Thus, the interaction of the membrane with viruses is of pure electrostatic nature and misses out on the possibility to mimic specific biological interactions.

Heparan sulfate is a prominent example for such specific interactions between a surface and viruses. It is a highly charged biomacromolecule that is present on cell surfaces and is used by several virus species as a mediator for infection.[13–15] Inspired by the specific effects of heparan sulfate, as well as its soluble analogue heparin, several synthetic polymers have been developed that mimic their structure and function.[16,17] Polyglycerol sulfates (PGS) have been shown to inhibit virus species that rely on heparan sulfate interactions, for example, herpes simplex virus type 1 (HSV-1)[18–20] and herpes simplex virus type 2 (HSV-2),[21] as well as respiratory syncytial virus[21] and SARS-CoV-2.[22] The synthetic polymers were even more potent inhibitors than heparin.[23] Hence, functionalizing material surfaces with PGS structures may be a useful approach to achieve a high binding efficiency for certain virus species.

Two coating strategies may be applicable to immobilize PGS on the surface of a filtration device (Figure 1):

First, a method that allows the simple surface functionalization with linear PGS (lPGS) has been described recently.[24] This method utilizes benzophenone groups as hydrophobic anchor that allows the adsorption on polymer surfaces. After adsorption to the surface, the benzophenone groups can be cured by UV light to form radicals and crosslink with the surface. Specifically, a triplet state in the carbonyl group is obtained after UV absorption and intersystem crossing. Unpaired electrons on the carbonyl then react with aliphatic hydrocarbons by abstracting hydrogen atoms and recombination with the resulting radicals on the surface. As a result, a dense layer of lPGS brushes is obtained.

Second, mussel inspired surface chemistry has proven itself a valuable tool for the functionalization of substrates.[25] Polymers as well as small molecules combining catechol and amine functionalities are capable of self-polymerization in aqueous solutions.[26,27] Thereby, catechol groups are oxidized to quinones under slightly basic conditions by oxygen dissolved in the solution, and can polymerize in dehydrogenative C—C bond formation reactions.[28,29] Surfaces that are immersed in the polymerizing solution will readily be coated with the respective substance, independent of the material of the surface. Such surface coatings can then be post-functionalized, since quinones can react with nucleophiles like amines or thiols in Michael type addition reactions, or by forming Schiff bases with amines.[30,31] Thus, lPGS may be introduced to any surface if it can be combined with amines.

In this study, we establish techniques to immobilize lPGS on a cheap and accessible filter material, that is, on a meltblown polypropylene fleece. The benzophenone-based approach as well as two mussel inspired approaches are tested and compared. These filtration materials then will serve for a highly specific adsorption of viruses from aqueous environments.

The mussel inspired approaches used in this study are based on either dopamine, which has been discussed extensively in literature,[26,31–33] or on MIdPG, which has been developed as alternative with a more rapid coating process and higher biocompatibility than dopamine (Figure 1a).[27,30,34] Postfunctionalisation is done with a new block copolymer consisting of an lPGS block and a short anchor block with amino side chains (Figure 1b). The benzophenone containing block copolymer will be introduced to the surface as described previously (Figure 1c).

The coated filter materials are analyzed in detail by performing contact angle measurements, electron microscopy and detection of charges with a charged dye. Furthermore, the interactions of coated fleece with proteins and two virus species is tested.

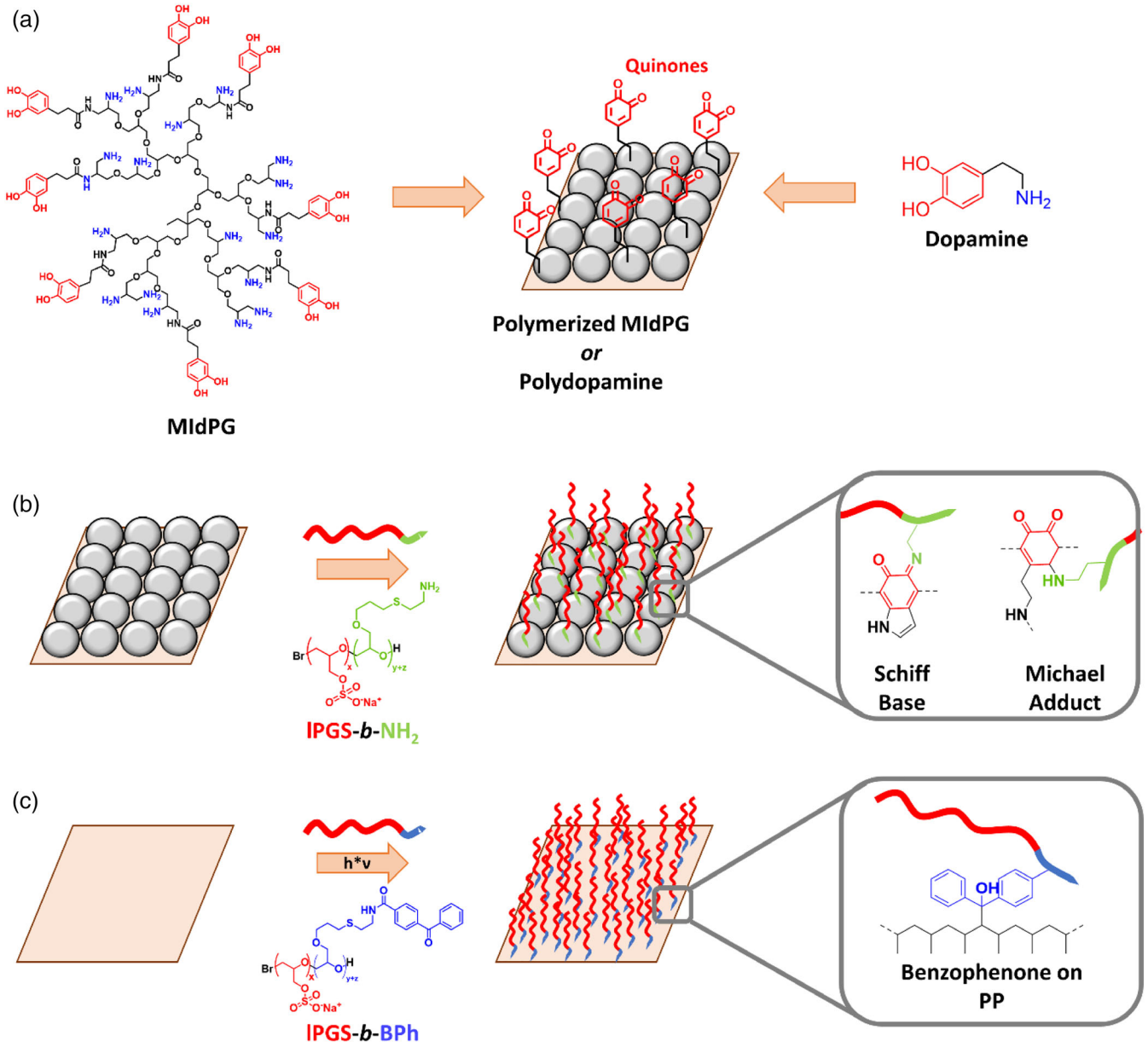

FIGURE 1 Description of methods for the immobilization of lPGS on a surface. (a) Mussel inspired dendritic polyglycerol or dopamine can polymerize onto a surface, forming an adhesion layer. That layer exhibits quinone groups which can be post-functionalized. (b) Amine carrying molecules can bind covalently to the adhesion layers by undergoing Michael addition or formation of Schiff bases with the quinone groups. This may be used to anchor a block copolymer consisting of linear polyglycerol sulfate and an amine carrying block on the adhesion layer. (c) The block copolymer lPGS-*b*-BPh carries a benzophenone anchor, which can directly interact with polymer surfaces and undergo radical reactions with the surface upon UV irradiation [Color figure can be viewed at wileyonlinelibrary.com]

2 | RESULTS AND DISCUSSION

2.1 | Coating approaches for lPGS on fleece samples

Meltblown polypropylene fleece samples were coated by three different approaches (Figure 2a,b). In the first approach, they were immersed in a solution of lPGS-*b*-BPh with guanidinium chloride (GHCl) for 10 min and then irradiated with UV light.[24] In the other two approaches, they were immersed in a polymerizing solution of either dopamine or MIdPG for 24 h or 1 h, respectively, and then treated with a solution of lPGS-*b*-NH_2 for 24 h at an elevated temperature of 80°C.

The coating procedures change the hydrophobicity of the fleece materials, as observed in contact angle measurements (Figure 2c). Untreated meltblown PP fleece is hydrophobic and minimizes the contact area between

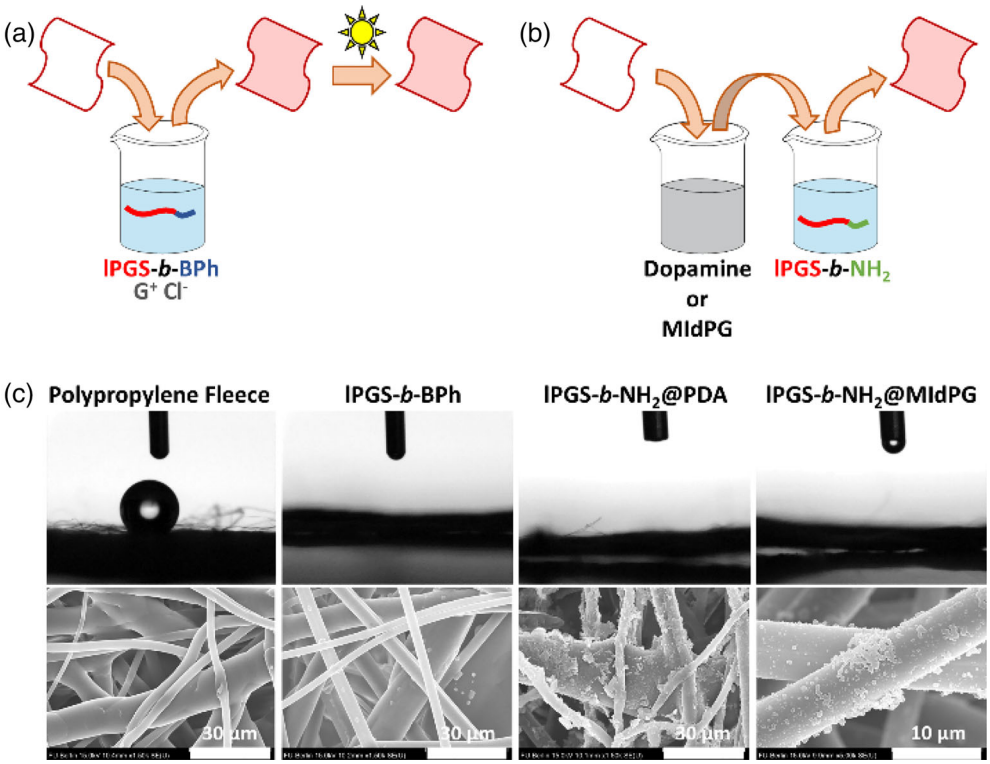

FIGURE 2 Schematic depiction of the coating processes and respective contact angle and electron microscopy images. (a) The dip coating procedure for lPGS-*b*-BPh requires a simple incubation of the fleece in polymer solution with guanidinium chloride (G^+Cl^-), followed by UV light irradiation. (b) Dopamine or mussel inspired dendritic polyglycerol (MIdPG) based coatings require two steps. First, the fleece is incubated in the respective solution for the adhesion layer, then washed and dried. Subsequently, the samples are post-functionalized with lPGS-*b*-NH_2 to produce lPGS-*b*-NH_2 on polydopamine (PDA) or MIdPG, respectively (lPGS-*b*-NH_2@PDA and lPGS-*b*-NH_2@MIdPG). (c) Contact angle and scanning electron microscopy (SEM) images. Untreated meltblown polypropylene fleece is hydrophobic and repels the water droplet. The coated samples become hydrophilic and soak up water droplets immediately. Both adhesion layers are visible as micrometer sized aggregates in electron microscopy images, while lPGS-*b*-BPh as monolayer coating is not visible in SEM [Color figure can be viewed at wileyonlinelibrary.com]

fibers and a water droplet. Each coating procedure changed the fleece samples to hydrophilic and water droplets soak into the fleece.

Scanning electron microscopy (SEM) images were obtained to reveal morphological changes on the fiber surfaces. Since lPGS-*b*-BPh forms a monolayer of a few nanometers in thickness, no change is observed in that case. Dopamine and MIdPG coatings on the other hand form micrometer large aggregates that deposit on the fibers and are clearly visible in SEM images. Treatment with lPGS-*b*-NH_2 adds a thin functional layer that does not influence the macroscopic morphology. Further images are shown in Figures S1–S4.

Additional analytical data were obtained by measuring the surface elemental composition with X-ray photoelectron spectroscopy (XPS). The obtained data are summarized in Table 1 (also see Figure S5). Unmodified polypropylene fleece consists of only carbon and hydrogen. XPS does not quantify hydrogen atoms, thus the carbon content is determined to be close to 100%. PDA and MIdPG add oxygen as well as nitrogen to the surface. Small amounts of sulfur may originate from the used buffer, 3-(*N*-morpholino)propanesulfonic acid. Addition of lPGS-*b*-NH_2 or lPGS-*b*-BPh to the surface leads to significant amounts of sulfur, which provides evidence for the presence of the sulfated polymers on the surfaces.

Overall, all of the three tested procedures reliably yield coated fleece materials with lPGS present on the surface. Coating with lPGS-*b*-BPh potentially is the most promising method because of its easy and fast application. Thus, it may be suitable for possible applications.

2.2 | Detection of sulfate groups with methylene blue

Standard techniques for surface characterization, for example, atomic force microscopy, electron microscopy, ellipsometry, or quartz crystal microbalance, cannot be used to directly detect the lPGS coating on a complex

TABLE 1 Surface elemental composition from X-ray photoelectron spectroscopy spectra

Sample	C (at%)	O (at%)	N (at%)	S (at%)
PP Fleece	97.5	1.8	0.0	0.0
PDA	78.6	15.0	5.9	0.4[a]
MIdPG	85.5	10.2	2.8	1.0[a]
lPGS-*b*-NH_2 @PDA	72.2	19.3	4.0	2.9
lPGS-*b*-NH_2 @MIdPG	80.4	14.4	1.8	2.5
lPGS-*b*-BPh	78.6	9.6	8.7[b]	1.8

[a]Residual sulfur content may originate from the used buffer.
[b]High amount of nitrogen may result from remaining guanidinium salt.

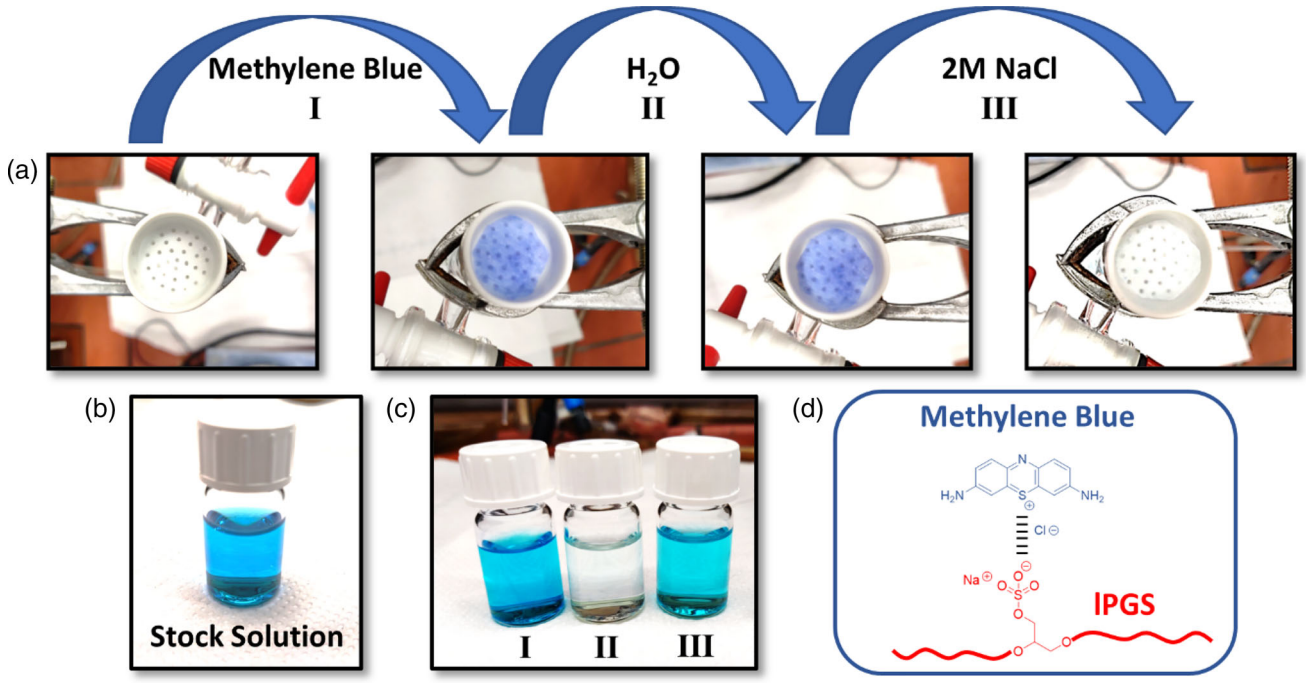

FIGURE 3 Filtration experiment to detect lPGS-*b*-BPh on coated fleece. (a) Step I: A solution of methylene blue is filtered through a sample of coated fleece. The dye is retained on the fleece, turning it blue. Step II: Washing with water does not remove the dye from the fleece. Step III: A 2 M salt solution can wash the dye off immediately. (b,c) Stock solution as well as washing solutions after each filtration step. (d) Schematic depiction of the ionic interaction between sulfate groups on lPGS and methylene blue [Color figure can be viewed at wileyonlinelibrary.com]

surface such as a fleece material. However, the applied coatings add a large amount of negatively charged sulfate groups to the surface. This feature will now be used to detect the polymers by measuring the adsorption of a positively charged dye to the respective surface.

Initially, a sample of lPGS-*b*-BPh coated fleece was tested in a filtration setup (Figure 3). When a solution of methylene blue in water was filtered through the sample, a portion of the dye was retained on the fleece, turning it blue (step I). Washing with water did not affect the color of the stained fleece (step II), but addition of 2 M sodium chloride immediately removed the dye from the fleece (step III). This demonstrates that the binding of methylene blue to the fleece surface is of electrostatic nature. At low salt concentration, the sodium counterions of the sulfate groups will be replaced by methylene blue ions. Adding an excess of salt causes charge screening, and methylene blue is released. Overall, an equilibrium exchange of the respective counterions is observed.

A qualitative comparison of coated and uncoated fleece samples further proved that lPGS is present on all fully functionalized samples (Figure 4a). In this experiment, fleece samples were incubated in a methylene blue solution (2.5 ml, 30 μM) for 2 h. The methylene blue concentration was determined before and after the incubation by UV/Vis spectroscopy. The difference was used to

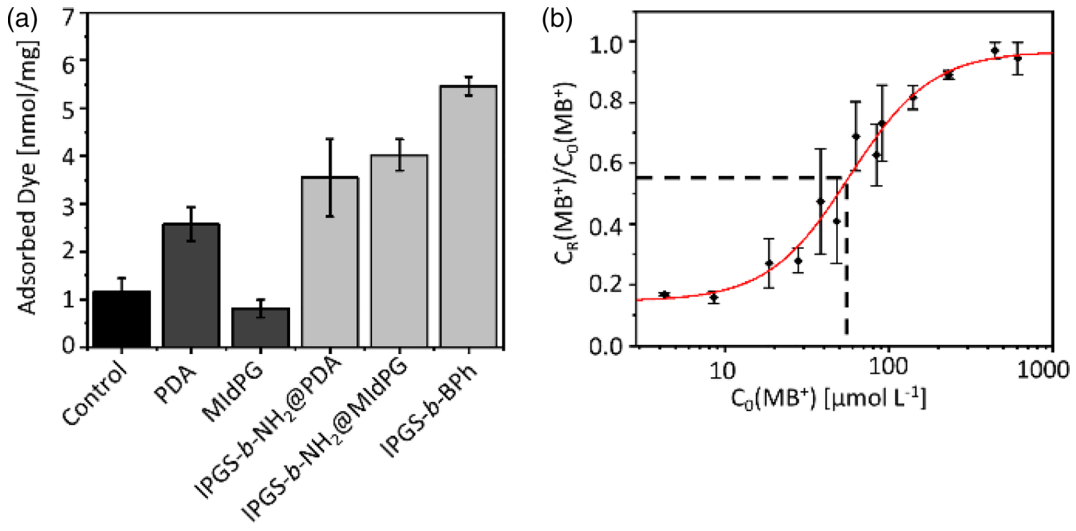

FIGURE 4 Quantitative analysis of methylene blue binding to coated fleece. (a) Amount of methylene blue bound to fleece samples, either with respective coating or uncoated control, normalized to the mass of the tested samples. (b) The adsorption isotherm for lPGS-*b*-BPh coated Meltblown fleece. The remaining dye concentration after incubation was normalized over the starting concentration for each concentration step. This ratio is plotted over the starting concentration [Color figure can be viewed at wileyonlinelibrary.com]

determine the amount of dye that has been adsorbed to the fleece. Furthermore, the obtained values were normalized to the mass of the respective fleece sample.

As shown in Figure 4a, uncoated samples adsorbed a low amount of methylene blue, which may be attributed to unspecific interactions between the hydrophobic dye and the polypropylene surface. The adhesion layer of polydopamine (PDA) increases the amount of adsorbed dye, likely due to interactions between the PDA surface and the aromatic system of methylene blue. This effect was not observed for MIdPG. All samples with lPGS coating bound substantially more methylene blue than the respective controls. This observation is especially pronounced for lPGS-*b*-NH_2@MIdPG and lPGS-*b*-BPh, while lPGS-*b*-NH_2@PDA adsorbed little more than PDA alone, owing to the high adsorption on PDA.

A quantitative analysis of the methylene blue adsorption was performed exemplarily for lPGS-*b*-BPh (Figure 4b). The incubation with methylene blue was performed at different dye concentrations. The adsorption of methylene blue to lPGS coated surfaces is an equilibrium exchange of sodium counter ions against methylene blue (MB^+). Therefore, plotting the residual dye concentration $C_R(MB^+)$, normalized to the respective starting concentration $C_0(MB^+)$, over $C_0(MB^+)$ gives the adsorption isotherm.

The adsorption isotherm of methylene blue on coated meltblown polypropylene fleece allows an estimation of the coating density of lPGS-*b*-BPh on the fiber surface. The inflection point of this curve at $C_I = 57$ µM can be taken as the concentration of saturation. Thus, we estimate that at that point every sulfate group has one methylene blue counterion. The sulfate density on the surface is therefore $\sigma_{SO_4^-} = 7.5$ µmol g^{-1}, when the concentration reduction of 45% at C_I is taken into account as well as the volume of the dye solution and the mass of the used fleece samples. A detailed description of the calculation is given in the supporting information.

Furthermore, the average surface area per gram of fleece was determined by measuring fiber diameters from SEM images. Together with the known number of sulfate groups per polymer chain, this yields the coating density to be $\rho_{Polymer} \approx 0.1$ nm^{-2}. This rough estimate represents a sufficiently high coating density and suggests that a polymer brush coating is formed for lPGS-*b*-BPh.

2.3 | Optimizing the coating parameters for lPGS-*b*-BPh

Evidently, for potential large-scale applications or industrial processing, the coating procedure should be as short as possible. Thus, we utilized the adsorption of methylene blue to test how fast the coating with lPGS-*b*-BPh can be done without a reduction of the coating density. In that experiment, coating procedures have been performed by either varying the polymer incubation time or the UV irradiation time (Figure S6). The incubation time could be reduced to 1 min without observing significant changes in the adsorption capacity for methylene blue. The irradiation time could be reduced to 2 min before a reduced polymer attachment or less stable coating was

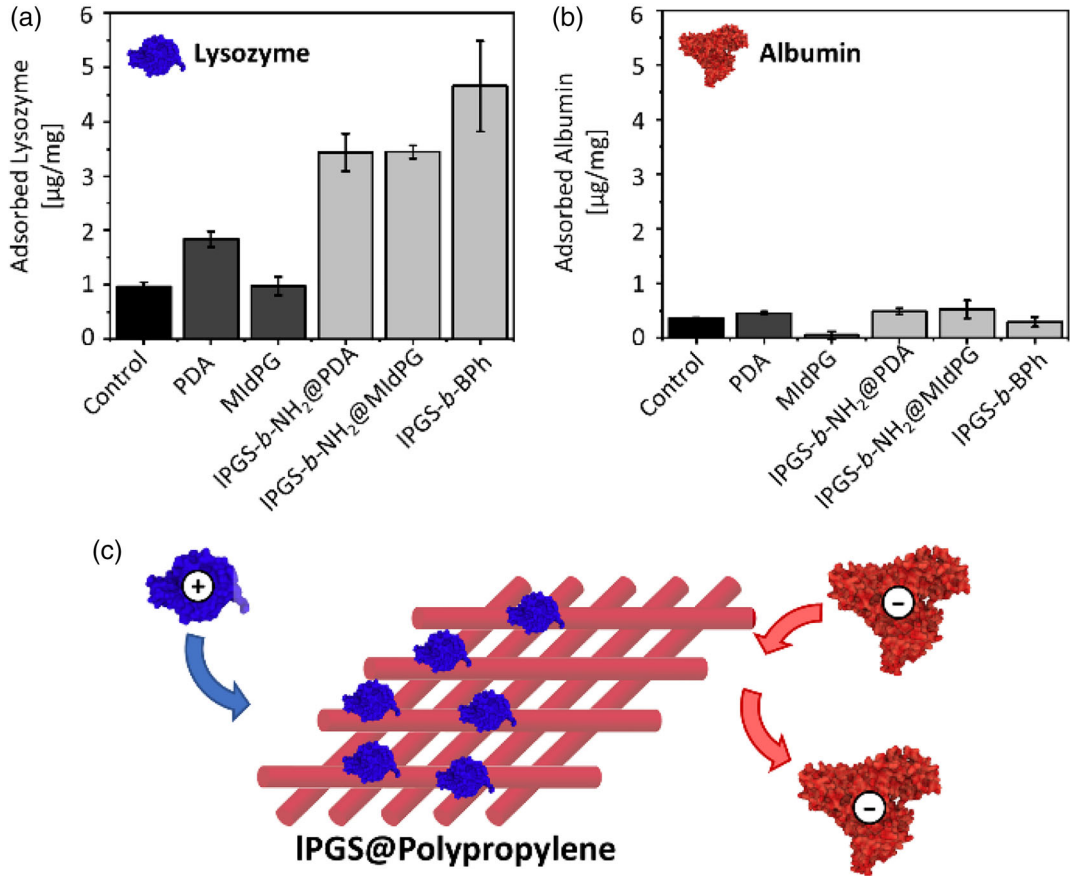

FIGURE 5 Protein adsorption data on coated polypropylene fleece. (a,b) The amount of lysozyme or human serum albumin adsorbed on fleece samples, normalized to the mass of the fleece samples. The fleeces with lPGS coatings strongly adsorb the positively charged protein lysozyme. Oppositely, the negatively charged protein HSA does not adsorb stronger to the coated fleece than to the untreated control. (c) Schematic representation of the interaction of the two protein species with coated polypropylene fibers. Lysozyme adsorbs to the fibers while HSA is being repelled due to electrostatic interactions. Protein structures were obtained from PDB (lysozyme: 3WUN; HSA: 4LB2) [Color figure can be viewed at wileyonlinelibrary.com]

observed. In total, the process may be accelerated to be performed within 3 min.

2.4 | Protein binding to coated surfaces is charge dependent

Next, the adsorption of proteins from solution was tested (Figure 5). Two protein species were chosen based on their net charge at physiological pH. Lysozyme as a small and positively charged protein, and human serum albumin (HSA) as overall negatively charged protein. The experiment was performed in analogy to the methylene blue adsorption. The virus concentration was determined using a Bradford assay, and the obtained values were normalized to the mass of the tested fleece samples.

Lysozyme exhibits low adsorption rates to uncoated and PDA or MIdPG coated materials. A high adsorption was observed for lPGS coatings, which is in good agreement to the literature.[24,35] Furthermore, the samples coated with lPGS-*b*-BPh adsorbed more lysozyme than the other two lPGS coated samples.

HSA did not exhibit significant adsorption to any of the tested fleece materials. Electrostatic repulsion between negative charges on HSA and sulfate groups on lPGS prevents the attachment of the protein to lPGS-coated surfaces. In contrast to our results, previously reported quartz crystal microbalance (QCM) experiments detected interactions between PGS coated QCM sensors and HSA.[24,36] However, QCM is a highly sensitive technique that can detect even weakest interactions between surface and proteins which cannot be observed in our experimental setting. Isothermal titration calorimetry experiments on the other hand did not detect interactions between dPGS and HSA at physiological pH and ionic strength, which is in agreement to our results.[37]

Overall, the adsorption of proteins to the coated fleece depends on electrostatic interactions between surface and

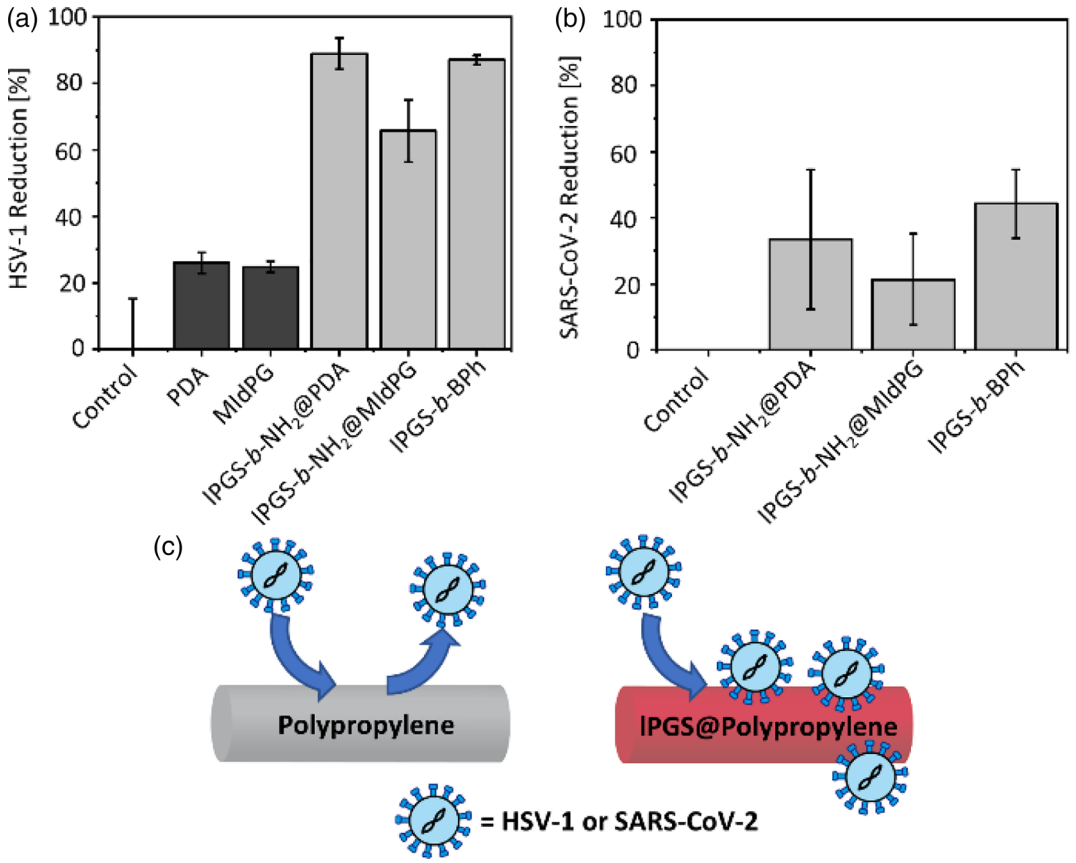

FIGURE 6 Virus capture from aqueous suspension. (a) HSV-1 or (b) SARS-CoV-2 suspensions were incubated with respective fleece materials and the reduction of the virus titer was measured. Values are given as relative reduction to positive control [Color figure can be viewed at wileyonlinelibrary.com]

proteins, and thus on the net charge of the protein. This is an important feature of the surface when it comes to the application of binding virus species, which will be tested in the following experiments.

2.5 | Virus capture from solution

After it was successfully demonstrated that small molecules as well as proteins bind to the coated fleece samples in a charge dependent manner, next we tested two virus strains that are known to bind to sulfated polymers (Figure 6).[18,22]

In this experiment, a suspension of either HSV-1 or SARS-CoV-2 was added to fleece samples and incubated for 1 h. The virus load of the suspension before and after incubation was determined via a plaque assay on Vero cells. Plaque forming units (PFU) per mL of suspension were calculated to yield the relative virus reduction after incubation.

HSV-1 binds efficiently to lPGS coated fleece, while the uncoated control as well as the PDA and MIdPG coated samples did not show a significant inhibition. lPGS-*b*-NH_2@PDA as well as lPGS-*b*-BPh achieved a reduction of plaque forming units of about 90%.

Subsequently, SARS-CoV-2 was tested. In this case, the inhibition with lPGS coated surface was lower than for HSV-1. The reduction of the virus titer was about 45% for lPGS-*b*-BPh on meltblown polypropylene. This observation is in good agreement to the half maximal inhibitory concentrations (IC50) reported for these virus species in literature. The value for lPGS on HSV-1 in solution was below 0.1 nanomolar,[18] while the value on SARS-CoV-2 was in the micromolar range.[22] This corresponds to a stronger inhibition of HSV-1 than SARS-CoV-2 by a factor of around 50,000 and explains well why HSV-1 is bound stronger to lPGS functionalized fleece than SARS-CoV-2.

3 | CONCLUSION

We developed three methods to coat polypropylene fleece with virus-binding polymers. First, two mussel-inspired approaches were utilized to create a dense layer of either PDA or MIdPG on the fiber surface. These

adhesion layers were then post-functionalized with the novel block-copolymer lPGS-*b*-NH_2. As third candidate, lPGS-*b*-BPh was applied directly on the fleece as nanometer thick surface coating. All coated fleece materials were characterized extensively using contact angle, SEM and XPS. Furthermore, the presence of sulfate groups was qualitatively and quantitatively analyzed by testing the adsorption of the positively charged dye methylene blue. This method could especially demonstrate that lPGS-*b*-BPh forms a dense coating on the fibers and thus it is present in the brush state.

Lysozyme and HSA served as two oppositely charged proteins that could demonstrate that biological substances will bind to the fleece depending on their overall charge. Finally, HSV-1 and SARS-CoV-2 were found to adsorb from a viral suspension to lPGS coated fleece materials. The efficiency of the virus experiments thereby reflected the different IC_{50} values reported in literature for lPGS on HSV-1 and SARS-CoV-2. The virus concentration could be reduced by about 90% for HSV-1, and by 45% for SARS-CoV-2.

All three coating procedures gave comparable results for methylene blue adsorption, protein adsorption and virus adsorption. However, lPGS-*b*-BPh stood out with slightly higher efficiencies in all experiments. Considering the simple and fast coating process (<5 min) for that polymer as compared to the other two methods (24–48 h), lPGS-*b*-BPh clearly is the most promising of the three tested coating methods.

4 | EXPERIMENTAL SECTION

4.1 | Materials

All chemicals and solvents obtained from commercial suppliers were used without further purification unless stated otherwise. Meltblown polypropylene fleece was obtained from commercial surgical masks. Dopamine hydrochloride, Lysozyme from chicken egg white and Human Serum Albumin were obtained from Sigma Aldrich (St. Louis, MO, USA). The Coomassie Plus Bradford Assay Kit was obtained from Thermo Scientific (MA, USA). UV irradiation during the coating procedure was done at 366 nm using a Camag laboratory UV lamp (Muttenz, Switzerland) at a constant distance with a power of 2.3 μW cm^{-2}.

4.2 | Synthesis of polymers

The synthesis of lPGS-*b*-BPh and MIdPG was performed as described in literature.[24,38] The novel polymer lPGS-*b*-NH_2 was synthesized analogous to the respective non-sulfated copolymer lPG-*b*-NH_2.[39] Complete descriptions of the synthetic procedures are given in the Supporting Information.

4.3 | General coating procedure with lPGS-*b*-BPh

Samples of polypropylene fleece were cut into pieces of about 2 cm × 2 cm.[24] The fleece was soaked briefly in ethanol to break the surface tension, then washed thoroughly with water and immediately soaked in an aqueous solution of guanidinium chloride (1.9 ml, 1 M) for 5 min. A stock solution of lPGS-*b*-BPh was added (0.1 ml, 2 mg ml^{-1}) to obtain a final polymer concentration of 0.1 mg ml^{-1} and a final salt concentration of 0.95 M. The fleece was incubated for 10 min in the dark, then taken from the solution and irradiated with UV light for 5 min on each side. The sample was washed thoroughly with PBS and with water and then dried at 60°C. For a more elaborate explanation of this coating method, the reader is referred to the cited literature.

4.4 | General coating procedure for dopamine

Fleece samples were placed in a fresh solution of dopamine hydrochloride (2 mg ml^{-1}) in MOPS buffer (3 ml, 0.1 M, pH = 7.5) and were incubated under constant shaking for 24 h. The fleece was then washed thoroughly with water and dried at 60°C.

4.5 | General coating procedure for MIdPG

Fleece samples were placed in a solution of MIdPG (2 mg ml^{-1}) in methanol (2 ml). The polymerization of MIdPG was initiated by adding MOPS buffer (0.7 ml, 0.1 M, pH = 8.5). After 1 h incubation, the fleece samples were washed thoroughly with water and dried at 60°C.

4.6 | Postfunctionalization with lPGS-*b*-NH_2

Fleece samples coated with either dopamine or MIdPG were placed in a solution of lPGS-*b*-NH_2 (1 mg ml^{-1}) in MOPS buffer (2 ml, 0.1 M, pH = 8.5).[30] The mixture was heated to 80°C for 24 h. Subsequently, the fleece samples were washed thoroughly with water and dried at 60°C.

4.7 | Contact angle

Contact angle measurements were performed using the contact angle goniometer OCA20 (Dataphysics Instruments, Filderstadt, Germany). A droplet of water (2 µl) was gently placed on the respective surface and allowed to equilibrate for 10 s. The shape of the droplet was recorded and evaluated using the software SCA20 (Dataphysics Instruments, Filderstadt, Germany). Contact angle values were not determined due to the uneven texture of fleece surfaces.

4.8 | Scanning electron microscopy

Fleece samples for SEM imaging were pretreated by sputtering with gold to obtain a conductive layer of at least 5 nm, using a compact coating unit CCU-010 by Safematic GmbH (Bad Ragaz, Switzerland). Images were obtained using an SU8030 field-emission scanning electron microscope (FE-SEM) by Hitachi (Tokyo, Japan). The accelerating voltage (Vac) was set to 20 kV, the current to 20 µA, and the working distance was 21.6 cm.

4.9 | X-ray photoelectron spectroscopy

X-ray photoelectron spectroscopy (XPS) spectra were recorded on a Kratos (Manchester, UK) Axis Ultra DLD spectrometer, equipped with a monochromatic Al Kα X-ray source. The spectra were measured in normal emission, and a source-to-sample angle of 60° was used. All spectra were recorded utilizing the fixed analyzer transmission (FAT) mode. The binding energy scale of the instrument was calibrated, following a technical procedure provided by Kratos Analytical Ltd (calibration was performed according to ISO 15472). The spectra were recorded utilizing the instrument's slot and hybrid lens modes. An analysis area of approximately 300 µm × 700 µm was investigated; charge neutralization was applied. For quantification, the survey spectra were measured with a pass energy of 80 electron volt (eV), and the spectra were quantified utilizing the empirical sensitivity factors that were provided by KRATOS (the sensitivity factors were corrected with the transmission function of the spectrometer).

4.10 | UV/Vis measurements

UV/Vis spectroscopy was used to analyze the concentrations of methylene blue and Coomassie-stained proteins. Methylene blue was measured at its absorption band maximum at 665 nm, while the Coomassie-protein complex showed an absorption maximum at 595 nm. Calibration curves were obtained from serial dilutions of known concentration for the dye and each protein. Absorbance values were only measured in a concentration range of 0–10 µmol L^{-1} for methylene blue, and 0–10 µg ml^{-1} for proteins. Samples with higher concentration were diluted to meet the required concentration range. Spectra were recorded using a Cary 8454 spectrometer (Agilent, CA, USA).

4.11 | Methylene blue adsorption

Fleece samples were immersed in 2.5 ml of a methylene blue solution in water at room temperature for 2 h. The initial dye concentration was determined by UV/Vis analysis. A sample of the supernatant was taken after incubation, diluted to meet the concentration range required for UV/Vis measurements, and the concentration was determined. The difference of starting concentration and final concentration was used to determine the amount of methylene blue adsorbed on the fleece. The obtained values were normalized to the mass of the respective fleece sample. In case of the adsorption isotherm, where normalizing to the fleece mass is not possible, all fleece samples were weighed to have the same weight of 8.5 mg.

4.12 | Protein adsorption

Protein adsorption experiments were performed analogous to the methylene blue adsorption experiments. Proteins were dissolved in PBS (30 µg ml^{-1} for lysozyme, 10 µg ml^{-1} for albumin). The Bradford assay was used for quantification by mixing the respective protein solution with a commercial Bradford assay kit in a 1:1 ratio. UV/Vis spectra were measured 5 min after mixing.

4.13 | Adsorption of HSV-1

The GFP-tagged HSV-1[18,40] (kindly provided by Dr. Yasushi Kawaguchi, University of Tokyo, Japan) was propagated on Vero cells (ATCC CCL-81) for 2 days. The supernatant containing GFP-tagged HSV-1 virus was collected, and the number of infectious virus particles (virus titer) in the supernatant was assessed using a plaque assay on Vero cells. The number of plaques per well was assessed using an epifluorescence microscope (Zeiss AxioVert 100) using the GFP channel and the virus titer of the initially added solution was calculated and is expressed as plaque-forming units (PFU)/ml.

To determine the adsorption of virus to coated fleece materials, samples of equal weight were disinfected with 75% EtOH for 10 min, washed with 0.5 ml DMEM medium for 15 min, and then incubated with 0.5 ml HSV-1 suspension (approx. 5×10^4 PFU ml^{-1}) for 1 h. The virus in the supernatant was then titrated in a plaque assay on Vero cells.

4.14 | Adsorption of SARS-CoV-2

SARS-CoV-2 München (SARS-CoV2M; BetaCoV/Germany/BavPat1/2020) was propagated on Vero E6 cells and quantified in a plaque assay.[22] Plaques were made visible by fixing the cells with 4% formaldehyde and staining with 0.75% crystal violet (aqueous solution) to make plaques visible. The experiments were performed in a BSL3 laboratory at the Institut für Virologie, Freie Universität Berlin.

The adsorption of SARS-CoV-2 to coated fleece materials was performed in an equal procedure as for HSV-1.

AUTHOR CONTRIBUTIONS

Maiko Schulze: Conceptualization (equal); investigation (lead); writing – original draft (lead); writing – review and editing (lead). **Chuanxiong Nie:** Investigation (equal); writing – original draft (supporting); writing – review and editing (supporting). **Greta Hartmann:** Investigation (supporting). **Philip Nickl:** Investigation (supporting); writing – original draft (supporting). **Michaël W. Kulka:** Investigation (supporting). **Matthias Ballauff:** Conceptualization (equal); supervision (equal); writing – original draft (supporting). **Rainer Haag:** Conceptualization (equal); funding acquisition (lead); resources (lead); supervision (lead); writing – review and editing (supporting).

ACKNOWLEDGMENTS

The authors thank D. Kutifa for the synthesis of lPG-*b*-NH_2. We thank J. M. Adler, J. Trimpert, and Prof. Benedikt Kaufer for their support in the SARS-CoV-2 incubation experiments. The assistance of the BioSupraMol core facility (located at the Freie Universität Berlin) is acknowledged for the characterization of the used polymeric materials. The authors gratefully than the BMBF for financial support in the project PathoClear (grant 13GW0544E). Open Access funding enabled and organized by Projekt DEAL.

DATA AVAILABILITY STATEMENT

The data that support the findings of this study are available in the supplementary material of this article.

ORCID

Rainer Haag https://orcid.org/0000-0003-3840-162X

REFERENCES

[1] H. Ritchie, E. Mathieu, L. Rodés-Guirao, C. Appel, C. Giattino, E. Ortiz-Ospina, J. Hasell, B. Macdonald, D. Beltekian, M. Roser, Coronavirus Pandemic (COVID-19), https://ourworldindata.org/coronavirus. Accessed: May **2022**.

[2] H. Wang, K. R. Paulson, S. A. Pease, S. Watson, H. Comfort, P. Zheng, A. Y. Aravkin, C. Bisignano, R. M. Barber, T. Alam, J. E. Fuller, E. A. May, D. P. Jones, M. E. Frisch, C. Abbafati, C. Adolph, A. Allorant, J. O. Amlag, B. Bang-Jensen, G. J. Bertolacci, S. S. Bloom, A. Carter, E. Castro, S. Chakrabarti, J. Chattopadhyay, R. M. Cogen, J. K. Collins, K. Cooperrider, X. Dai, W. J. Dangel, F. Daoud, C. Dapper, A. Deen, B. B. Duncan, M. Erickson, S. B. Ewald, T. Fedosseeva, A. J. Ferrari, J. J. Frostad, N. Fullman, J. Gallagher, A. Gamkrelidze, G. Guo, J. He, M. Helak, N. J. Henry, E. N. Hulland, B. M. Huntley, M. Kereselidze, A. Lazzar-Atwood, K. E. LeGrand, A. Lindstrom, E. Linebarger, P. A. Lotufo, R. Lozano, B. Magistro, D. C. Malta, J. Månsson, A. M. M. Herrera, F. Marinho, A. H. Mirkuzie, A. T. Misganaw, L. Monasta, P. Naik, S. Nomura, E. G. O'Brien, J. K. O'Halloran, L. T. Olana, S. M. Ostroff, L. Penberthy, R. C. Reiner Jr., G. Reinke, A. L. P. Ribeiro, D. F. Santomauro, M. I. Schmidt, D. H. Shaw, B. S. Sheena, A. Sholokhov, N. Skhvitaridze, R. J. D. Sorensen, E. E. Spurlock, R. Syailendrawati, R. Topor-Madry, C. E. Troeger, R. Walcott, A. Walker, C. S. Wiysonge, N. A. Worku, B. Zigler, D. M. Pigott, M. Naghavi, A. H. Mokdad, S. S. Lim, S. I. Hay, E. Gakidou, C. J. L. Murray, *Lancet* **2022**, *6736*, 1.

[3] M. V. A. Corpuz, A. Buonerba, G. Vigliotta, T. Zarra, F. Ballesteros, P. Campiglia, V. Belgiorno, G. Korshin, V. Naddeo, *Sci. Total Environ.* **2020**, *745*, 140910.

[4] H. Lee, M. Kim, S. Y. Paik, C. H. Lee, W. H. Jheong, J. Kim, G. P. Ko, *J. Water Health* **2011**, *9*, 27.

[5] L. Maunula, K. Söderberg, H. Vahtera, V. P. Vuorilehto, C. H. Von Bonsdorff, M. Valtari, T. Laakso, K. Lahti, *J. Water Health* **2012**, *10*, 87.

[6] F. G. Masclaux, P. Hotz, D. Friedli, D. Savova-Bianchi, A. Oppliger, *Water Res.* **2013**, *47*, 5101.

[7] I. Ouardani, S. Turki, M. Aouni, J. L. Romalde, *Appl. Environ. Microbiol.* **2016**, *82*, 3834.

[8] I. Bar-Or, K. Yaniv, M. Shagan, E. Ozer, M. Weil, V. Indenbaum, M. Elul, O. Erster, E. Mendelson, B. Mannasse, R. Shirazi, E. Kramarsky-Winter, O. Nir, H. Abu-Ali, Z. Ronen, E. Rinott, Y. E. Lewis, E. Friedler, E. Bitkover, Y. Paitan, Y. Berchenko, A. Kushmaro, *Front. Public Health* **2022**, *9*, 1.

[9] S. Westhaus, F. A. Weber, S. Schiwy, V. Linnemann, M. Brinkmann, M. Widera, C. Greve, A. Janke, H. Hollert, T. Wintgens, S. Ciesek, *Sci. Total Environ.* **2021**, *751*, 141750.

[10] G. La Rosa, M. Iaconelli, P. Mancini, G. Bonanno Ferraro, C. Veneri, L. Bonadonna, L. Lucentini, E. Suffredini, *Sci. Total Environ.* **2020**, *736*, 139652.

[11] H. Shi, E. V. Pasco, V. V. Tarabara, *Environ. Sci. Water Res. Technol.* **2017**, *3*, 778.

[12] S. Bofill-Mas, M. Rusiñol, *Curr. Opin. Environ. Sci. Health* **2020**, *16*, 7.

[13] V. Cagno, E. D. Tseligka, S. T. Jones, C. Tapparel, *Viruses* **2019**, *11*, 1.

[14] T. M. Clausen, D. R. Sandoval, C. B. Spliid, J. Pihl, H. R. Perrett, C. D. Painter, A. Narayanan, S. A. Majowicz, E. M. Kwong, R. N. McVicar, B. E. Thacker, C. A. Glass, Z. Yang, J. L. Torres, G. J. Golden, P. L. Bartels, R. N. Porell, A. F. Garretson, L. Laubach, J. Feldman, X. Yin, Y. Pu, B. M. Hauser, T. M. Caradonna, B. P. Kellman, C. Martino, P. L. S. M. Gordts, S. K. Chanda, A. G. Schmidt, K. Godula, S. L. Leibel, J. Jose, K. D. Corbett, A. B. Ward, A. F. Carlin, J. D. Esko, *Cell* **2020**, *183*, 1043.

[15] M. Koehler, M. Delguste, C. Sieben, L. Gillet, D. Alsteens, *Annu. Rev. Virol.* **2020**, *7*, 143.

[16] S. J. Paluck, T. H. Nguyen, H. D. Maynard, *Biomacromolecules* **2016**, *17*, 3417.

[17] C. Cheng, S. Sun, C. Zhao, *J. Mater. Chem. B* **2014**, *2*, 7649.

[18] P. Pouyan, C. Nie, S. Bhatia, S. Wedepohl, K. Achazi, N. Osterrieder, R. Haag, *Biomacromolecules* **2021**, *22*, 1545.

[19] V. Ahmadi, C. Nie, E. Mohammadifar, K. Achazi, S. Wedepohl, Y. Kerkhoff, S. Block, K. Osterrieder, R. Haag, *Chem. Commun.* **2021**, *57*, 11948.

[20] B. Ziem, W. Azab, M. F. Gholami, J. P. Rabe, N. Osterrieder, R. Haag, *Nanoscale* **2017**, *9*, 3774.

[21] E. Mohammadifar, M. Gasbarri, V. Cagno, K. Achazi, C. Tapparel, R. Haag, F. Stellacci, *Biomacromolecules* **2022**, *23*, 983.

[22] C. Nie, P. Pouyan, D. Lauster, J. Trimpert, Y. Kerkhoff, G. P. Szekeres, M. Wallert, S. Block, A. K. Sahoo, J. Dernedde, K. Pagel, B. B. Kaufer, R. R. Netz, M. Ballauff, R. Haag, *Angew. Chem. Int. Ed.* **2021**, *60*, 15870.

[23] C. Nie, A. K. Sahoo, R. R. Netz, A. Herrmann, M. Ballauff, R. Haag, *ChemBioChem* **2022**, *23*, 23.

[24] M. Schulze, S. Adigüzel, P. Nickl, A. Schmitt, J. Dernedde, M. Ballauff, R. Haag, *Adv. Mater. Interfaces* **2022**, *9*, 2102005.

[25] Y. Liu, K. Ai, L. Lu, *Chem. Rev.* **2014**, *114*, 5057.

[26] H. Lee, S. M. Dellatore, W. M. Miller, P. B. Messersmith, *Science* **2007**, *318*, 426.

[27] Q. Wei, K. Achazi, H. Liebe, A. Schulz, P.-L. M. Noeske, I. Grunwald, R. Haag, *Angew. Chem. Int. Ed.* **2014**, *53*, 11650.

[28] F. Yu, S. Chen, Y. Chen, H. Li, L. Yang, Y. Chen, Y. Yin, *J. Mol. Struct.* **2010**, *982*, 152.

[29] J. Liebscher, R. Mrówczyński, H. A. Scheidt, C. Filip, N. D. Hădade, R. Turcu, A. Bende, S. Beck, *Langmuir* **2013**, *29*, 10539.

[30] M. W. Kulka, I. S. Donskyi, N. Wurzler, D. Salz, Ö. Özcan, W. E. S. Unger, R. Haag, *ACS Appl. Biomater.* **2019**, *2*, 5749.

[31] S. Heinen, S. Rackow, J. L. Cuellar-Camacho, I. S. Donskyi, W. E. S. Unger, M. Weinhart, *J. Mater. Chem. B* **2018**, *6*, 1489.

[32] H. Lee, N. F. Scherer, P. B. Messersmith, *Proc. Natl. Acad. Sci.* **2006**, *103*, 12999.

[33] I. S. Kwon, C. J. Bettinger, *J. Mater. Chem. B* **2018**, *6*, 6895.

[34] C. Schlaich, M. Li, C. Cheng, I. S. Donskyi, L. Yu, G. Song, E. Osorio, Q. Wei, R. Haag, *Adv. Mater. Interfaces* **2018**, *5*, 1701254.

[35] Q. Ran, X. Xu, J. Dzubiella, R. Haag, M. Ballauff, *ACS Omega* **2018**, *3*, 9086.

[36] D. D. Stöbener, F. Paulus, A. Welle, C. Wöll, R. Haag, *Langmuir* **2018**, *34*, 10302.

[37] Q. Ran, X. Xu, P. Dey, S. Yu, Y. Lu, J. Dzubiella, R. Haag, M. Ballauff, *J. Chem. Phys.* **2018**, *149*, 163324.

[38] M. W. Kulka, S. Smatty, F. Hehnen, T. Bierewirtz, K. Silberreis, C. Nie, Y. Kerkhoff, C. Grötzinger, S. Friedrich, L. I. Dahms, J. Dernedde, I. Grunwald, M. Schirner, U. Kertzscher, K. Affeld, R. Haag, *Adv. Mater. Interfaces* **2020**, *7*, 2000272.

[39] L. Yu, C. Cheng, Q. Ran, C. Schlaich, P. L. M. Noeske, W. Li, Q. Wei, R. Haag, A. C. S. Appl, *Mater. Interfaces* **2017**, *9*, 6624.

[40] I. S. Donskyi, W. Azab, J. L. Cuellar-Camacho, G. Guday, A. Lippitz, W. E. S. Unger, K. Osterrieder, M. Adeli, R. Haag, *Nanoscale* **2019**, *11*, 15804.

SUPPORTING INFORMATION

Additional supporting information can be found online in the Supporting Information section at the end of this article.

How to cite this article: M. Schulze, C. Nie, G. Hartmann, P. Nickl, M. W. Kulka, M. Ballauff, R. Haag, *J. Appl. Polym. Sci.* **2023**, *140*(6), e53444. https://doi.org/10.1002/app.53444